

## Effect of Silver Composition on Electrochemical Degradation of AlZn Alloy

S. Valdez<sup>1,\*</sup>, M.I. Pech-Canul<sup>2</sup>, J.A. Ascencio-Gutiérrez<sup>1</sup>, S.R. Casolco<sup>3</sup>

<sup>1</sup>Instituto de Ciencias Físicas-UNAM, Av. Universidad 1001, Col. Chamilpa, 062210, Cuernavaca, Morelos, México

<sup>2</sup>CINVESTAV-US. Carretera Saltillo-Monterrey Km13, Saltillo Coahuila, México

<sup>3</sup>Instituto Tecnológico y de Estudios Superiores de Monterrey, ITESM-Puebla, Vía Atlixcáyotl 2301, 72800. Puebla, Puebla, México

\*E-mail: [svaldez@fis.unam.mx](mailto:svaldez@fis.unam.mx)

Received: 2 May 2013 / Accepted: 10 June 2013 / Published: 1 July 2013

---

The chemical composition of metallic AlZnAg alloy is related with microstructure in order to know their influence on electrochemical degradation. The microstructure has been characterized by high transmission electron microscopy with energy-dispersive X-ray. The electrochemical behavior has been tested by potentiodynamic polarization tests. In addition, weight loss analysis was carried out for the corrosion rate. In electrochemical tests the results showed the significant influence of silver concentration on the dissolution reactions of Al-matrix, solid solution rich-Zn, and AgZn<sub>3</sub> precipitate phase. The electrochemical investigation shows that the corrosion rate increases with the silver additions. Likewise, it was moreover evidenced the development of a film passive layer for the maximum silver content alloys; the passivity of this cover could be broken due to the existence of precipitate phase AgZn<sub>3</sub>. Based on this behavior the AgZn<sub>3</sub> particles, and microstructural phases play a significant role in the corrosion process for the metallic AlZn alloys

---

**Keywords:** AlZnAg alloy, potentiodynamic test, AgZn<sub>3</sub> particulates, corrosion rate.

### 1. INTRODUCTION

Metallic alloys processing involves the solidification from the melt as an essential step in manufacturing products. When the alloyed melt has cooled below the equilibrium liquidus temperature  $T_m$ , the heterogeneous nucleation occurs. This process could be influenced by the presence of soluble solutes, and the existence of suitable insoluble substrates in the metallic melts. In addition, solidification process can occur in practice, depending on alloying elements, alloy composition, casting

size, and undercooled liquid [1]. The importance of chemistry composition, understood as solute concentration, or microconstituents composition, was demonstrated by W.A. Tiller et al. in the constitutional supercooling criterion [2]. This theory has been developed to predict the solidification microstructure. The literature contains many papers dedicated to the study of microstructure as an important role in the alloys properties [3,4,5]. In addition, chemical composition, as a part of material property, influences the solidification microstructure, and is evidence of the existence of interactions, for materials performance, between three main parameters: (i) microstructure, (ii) growth related to its surroundings, and (iii) properties [6]. Knowing how a chemical property on metallic materials act as a function of corrosion resistance is important to predict the electrochemical attributes of an alloy during their corrosion process. With all this in mind, our purpose now was to determine the relationship between electrochemical parameters, chemical composition and microstructure of the AlZn alloys.

The Aluminium (Al) based alloys mixture with Zinc (Zn) is one of the leading candidates for many end-use applications, due to their attractive physical, mechanical, and superplastic properties in conjunction with good abrasion and wear resistances [7]. The influence of silver (Ag) solute to binary AlZn alloys act to exert a marked effect on their grain structure and microstructural characteristics [8]. Nevertheless, the electrochemical mechanism by which Ag is related with the corrosion behavior of these alloys has not been studied.

Other beneficial effect of silver is the dimensional stability on the AlZn alloys; on contrary, of copper, which is another solute used as alloying candidate, however copper causes dimensional instability. At a copper content of 0.06%, Al-Zn alloy increases tensile strength, creep strength and corrosion resistance [9]. Other chemical elements, such as Cr, Mn and Zr are generally added to control grain structure and weldability, mainly [10]. Even though the extensive investigations of the chemical properties, such as solute concentration and microconstituents nature, few studies reported the corrosion behavior taking into account the effect of several microconstituents.

It is generally recognized that chemical composition and microstructure make major contributions to the mechanical properties, metallurgical features and corrosion behavior. In addition, the corrosion susceptibility as well as the corrosion resistance could enhance by processing methods in conjunction with microstructural modification [11].

Our purpose now, was to determine the influence of chemical composition with increasing of the solute silver content on the corrosion behavior of Al-Zn alloy. In addition, the present paper reports the correlation between microstructure with the electrochemical parameters of the AlZn-Xat.%Ag alloys. The corrosion behavior was deduced by potentiodynamic polarization curves, while microstructure has been determined by HRTEM at four Ag contents

## 2. EXPERIMENTAL PROCEDURE

The influence of different silver composition on the corrosion behavior, and microstructure of binary aluminium-zinc alloy has been studied. The study was carried out with the addition of four different Ag contents (0.5, 2.5, 3.5, and 4.5 wt %), as metallic element. The master alloys were made from 99.8% Al, and were added to zinc of the same purity.

The Al and Zn ingots pieces were inserted in a steel crucible, in a resistance electrical furnace at constant temperature of 700°C. In order to achieve better homogenization, molten Ag was directly added to the AlZn-melt alloy into the steel crucible via refractory feeder tip at 1150 rpm during 15 minutes. The AlZnAg melt was poured into a steel mold to form ingots of 100 mm x 150 mm x 20 mm. When the solidification was complete, a test sample is removed from the AlZnAg ternary ingots. Their nominal chemical composition was obtained by ICP showed in Table 1.

Metallographic specimen surfaces were prepared carefully by the standard technique of grinding with SiC up to 1000 grade emery papers and mechanical polishing with Al<sub>2</sub>O<sub>3</sub> suspension solution. A solution of three parts glacial acetic acid and one part of 100 volume hydrogen peroxide was used for chemical polishing. While etching reagent, used to reveal the microstructural phases, was prepared by dissolving 10 g ammonium molybdate and 25 g of citric acid in 100 ml of deionized water, and stirred for 3 min. Transmission electron microscopy (TEM) observations were performed using a JEM 2010F with an energy dispersive X-ray spectrometer (HP-GE-Detector, NORAN).

**Table 1.** Chemical compositions (wt. %) of AlZnAg alloys investigated

Alloy type	Al	Zn	Ag	Others
Ag1	21.334	78.15	0.50	0.016
Ag2	19.48	78.00	2.50	0.020
Ag3	18.272	78.21	3.50	0.018
Ag4	21.429	78.05	4.50	0.021

One electrochemical method explored in studying the corrosion behaviors of materials was a usual polarization curve measurement. In a polarization curves are indicated some corrosion events which corresponding with the observation on corrosion morphologies. With all this in mind, the electrochemical corrosion test was performed in a 1cm<sup>2</sup> squares area of samples, embedded in epoxy resin, which act as working electrodes. The exposed surface area was ground (600 grit SiC finish) sample. Afterwards, specimens were cleaned by immersion in a solution of 50 vol. % nitric acid (HNO<sub>3</sub>) for 3 min in accordance with ASTM Standard G31[12]. Finally, samples were dried in a hot stream air before measurements.

Potentiodynamic polarization tests were carried out with the specimens immersed in an aerated substitute ocean water electrolyte, prepared with analytical grade reagent NaCl, and deionized water, with an initial pH of 8.3 according to ASTM D1141 [13]. A corrosion cell kit using the three-electrode set-up with a saturated calomel reference electrode (SCE) used to measure the corrosion potential. While a platinum wire auxiliary electrode was used as counter electrode. Using an automatic data acquisition system the potentiodynamic current-potential curves were recorded by changing the working electrode potential from -700mv to +700mV at open-circuit potential (OCP), E<sub>corr</sub>, with 1 mVs<sup>-1</sup> scan rate at 22 °C. In order to determinate the current density i<sub>corr</sub>, the polarization resistance measured from the test was used in the Stearn-Geary equations [14] as shown in equations (2, and 3):

$$B = \frac{\beta_a \beta_c}{2.303(\beta_a + \beta_c)} \quad (1)$$

$$R_p = \left( \frac{\beta_a \beta_c}{2.303(\beta_a + \beta_c)} \right) \left( \frac{1}{i_{corr}} \right) \quad (2)$$

$$R_p = \frac{B}{i_{corr}} = \frac{(\Delta E)}{(\Delta i)_{\Delta E \rightarrow 0}} \quad (3)$$

The shape of the anodic and cathodic branches allows determine the anodic and cathodic Tafel slopes  $\beta_a$  and  $\beta_c$ . In consequence, by Eq. (1) the B constant can be calculated.  $R_p$  corresponds to the polarization resistance, that is, the ratio between the potential shift  $\Delta E$ , and the corresponding current change  $\Delta i$  in an experimental polarization test within a few millivolts of the corrosion potential.

For the case of weight lost test, the working electrode surface from every AlZn alloy was polished to 1000grit SiC paper, degreased in acetone; washed thoroughly in ethanol, and kept in a desiccator prior to immersion tests. A saline solution, 3.5 % NaCl, prepared from analytical reagent grade with deionized water was the electrolyte during 1, 3, 7, 14, and 28 at a room temperature. Subsequently, AlZn samples were removed, and chemically cleaned by immersion in a solution of 50 vol. % nitric acid for 3 min. in accordance with ASTM Standard G31 [12]. Each test was performed in duplicate.

### 3. RESULTS AND DISCUSSION

Potentiodynamic polarization curves shows characteristic regions correlated to active, active-passive, passive, and stable pitting events [15]. A similar behavior from those regions can be seen in the curve of the Figure 1 for AlZnAg alloys in 3.5% NaCl solution.

**Table 2.** Electrochemical parameters of AlZn alloys at different silver composition.

Alloy type	$E_{corr}$ (mV)	$i$ (mA/cm <sup>2</sup> )	$I_{corr}$ (mA/cm <sup>2</sup> )
Ag1	-1098	30647	3.8
Ag2	-1090	27688	6.1
Ag3	-1240	24049	10.7
Ag4	-1210	29586	12.3

Polarization curves are the relationship between the applied potential ( $E_{app}$ ) or driving force with current density ( $i$ ) generated with the working electrode AlZnAg, and the counter electrode. In our case, the corrosion potential ( $E_{corr}$ ) describe as the intersection between two polarization curves,

showed the lowest  $E_{\text{corr}}$  values close to -1200 mV for the AlZnAg with 3.5 and 4.5 wt% Ag; which are agree with an active-passive behavior identified along the anodic branch. To some extent, for the anodic branch the alloys with 2.5 and 0.5 wt% Ag content did not exhibit passive regions, only active dissolution with an  $E_{\text{corr}}$  value close to -1100 mV was detected (Table 2). Knowing the facts, of how the chemical composition of silver microconstituent has been influenced the passive, and active behavior; we can determine the alloy degradation.

It is well known that the intensity of the metallic electrochemical reaction is represented by the corrosion current density value,  $i_{\text{corr}}$ . As can be seen in table 2, for instance, in our metallic alloys, the  $i_{\text{corr}}$  is the highest value  $12.3 \mu\text{A}/\text{cm}^2$ , for the higher Ag content 4.5% Ag. While, the lowest  $i_{\text{corr}}$  value,  $3.8 \mu\text{A}/\text{cm}^2$ , relates to 0.5% Ag. Because of these differences the rate of anodic dissolution ( $i_{\text{corr}}$ ) reflects the formation of a passive film. In addition, such response is correlated with a passive current density values which became smaller as function of the silver chemical composition. Thus, it is more meaningful the beneficial effects of increasing the silver contents in AlZn alloys for the passive region formation.

As expected, at open circuit potentials (OCP) the corrosion rates increased. The OCP's values shifted to anodic direction. However, as the polarization increases, and the passive region were trespassed, it is shown that the anodic current density values were very similar for all alloys regardless the Ag content. This behavior suggests that corrosion process is diffusion-controlled through the formed corrosion products. This aqueous corrosion usually reflects that the alloy is exposed to a liquid electrolyte, inconsequence the electrochemical process occurs at the working electrode surface.

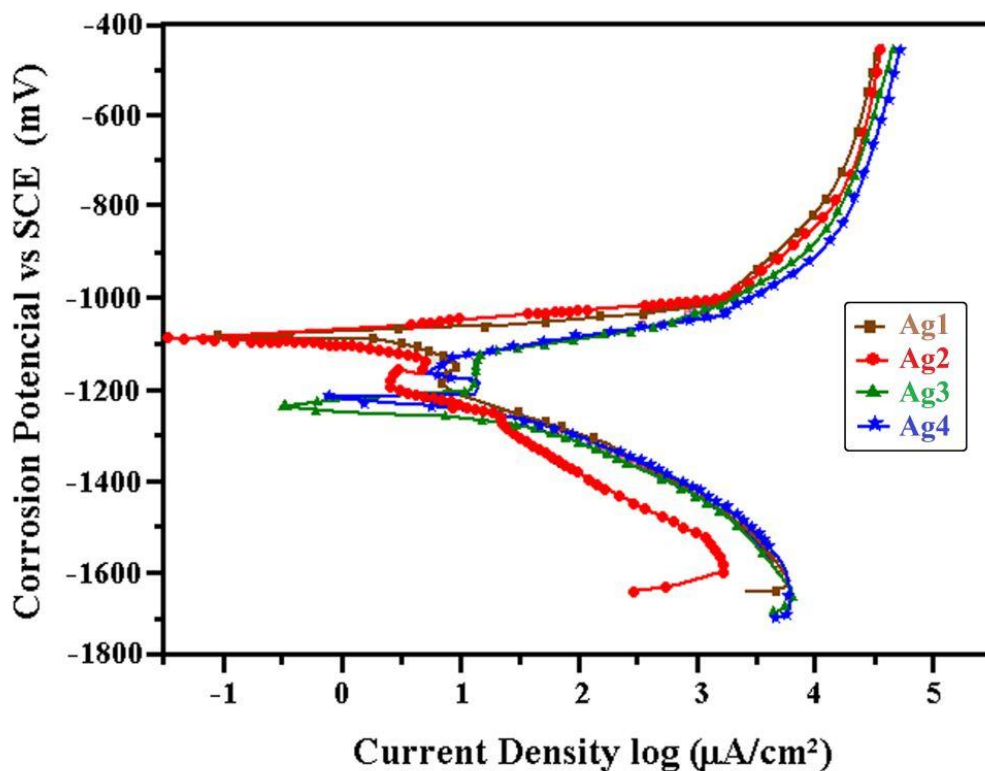


Figure 1. Potentiodynamic polarization curves for AlZnAg alloys in 3.5% NaCl

Therefore, these results evidence that the Ag chemical composition does not have a suppressing effect on the anodic reaction as Cr, Cu, Ni and Ca in steel does [16]. In a similar way, it was reported [17] that the increase on silicon content on AlSi alloys provides a deteriorate effect on the corrosion resistance. However, significantly combined parameters can affect the corrosion resistance. Electrochemical degradation is a dominant effect, which has often been related with grain boundaries, second phases, and inclusions [18].

The thermodynamic driving force for cathodic reactions can be evinced in the cathodic branch, such as illustrated in the potentiodynamic curve. The potential-current density curve reveals that the cathodic density currents were similar for each chemical composition of silver; although, the AlZn-2.5%Ag alloy showed the lowest value. It is generally accepted that in aerated saline media cathodic polarizations represents the oxygen reduction and hydrogen evolution reactions as can be seen in the equation 4 [19].



This cathodic reaction occurs depending on the pH, and dissolved oxygen concentration in the solution.

Based on the performance of electrochemical reaction, both oxidation and reduction reactions occur at different time interval. An efficient method to characterize the corrosion rate, which depends on the chemical kinetics, has been applied. Weight-loss measurement reflects a linear relationship between the alloy dissolution rate, and the corrosion current  $i_{\text{corr}}$  throughout the Faraday's law. The equation (5) simplifies the relationship in terms of corrosion rate (RM), while analogously the equation (6) expresses the electrochemical process according to the corrosion density in  $\text{A}/\text{cm}^2$  [20] g.

$$R_m = \frac{M}{nF\delta} i_{\text{corr}} \quad 5$$

$$i_{\text{corr}} = \frac{nF\Delta m}{MA t} \quad 6$$

Where, M is molecular weight of alloy in g/mol, n is the number of electrons exchanged in the dissolution reaction; F is Faraday's constant equal to 96,500 coulombs,  $\delta$  alloy density in  $\text{g}/\text{cm}^3$ ,  $\Delta m$  is weight loss due to corrosion in grams, t is time in seconds, A is the area of metallic alloy surface exposed to the corrosion in  $\text{cm}^2$ .

For the expression of this measurement results, the Figure 2 shows the dissolution rate of AlZnAg alloys, which have been immersed in 3.5 wt. % NaCl aqueous solution. For the four chemical concentrations of silver as microconstituent, the AZnAg alloys had a slow corrosion rate during the first 72 hours; afterwards, different electrochemical dissolution processes were achieved, which results in a metallic surface degradation.

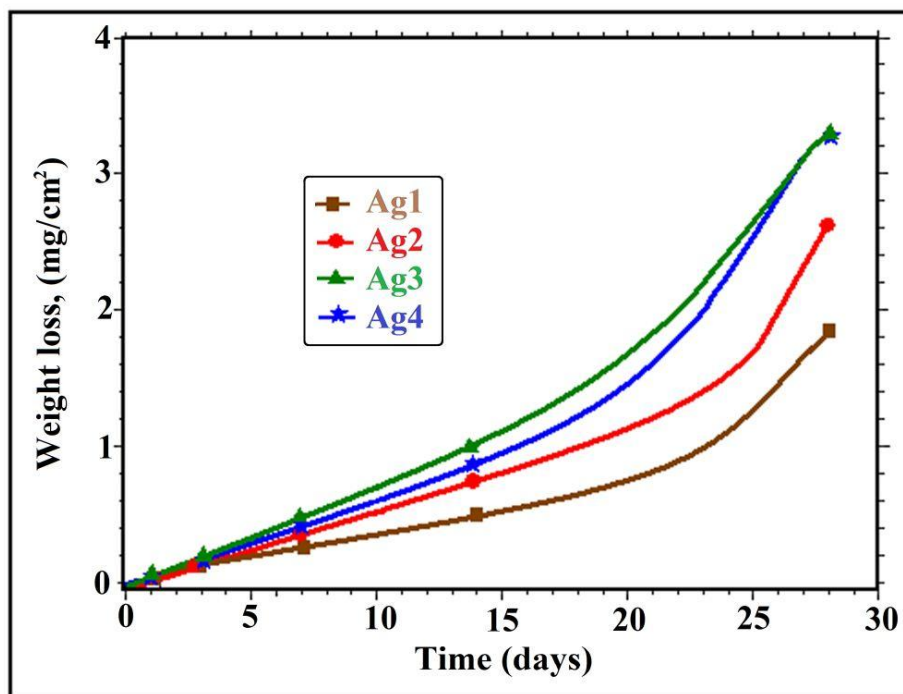


**Figure 2.** Weight loss estimation of AlZnAg alloys as a function of time in 3.5 wt. % NaCl solution.

The corrosion of AlZnAg samples, result in a loss of electrons. In consequence, the oxidation of AlZnAg alloy produces a corrosion rate, which increases as the Ag content and immersion times also increased. This is in agreement with the well-known statement that “internal structure of an alloy controls and modifies the nature and interaction type of the existing defects” [Error! Bookmark not defined.]. In our case, the alloy composition and metallurgical factors impacts the formation of  $\text{AgZn}_3$  particles. This precipitated phase seem to be responsible for the corrosion action due to the fact that they act as local anodes susceptible to localized corrosion. For general considerations, the precipitated phases and intermetallic particles can switch between anodic or cathodic relative to the matrix alloy as a result of selective electrochemical dissolution. In this case, the anodic  $\text{AgZn}_3$  particles represent sites for disruption of any air-formed oxide that covers the AlZnAg surface; as a consequence, the protective surface layer can be broken, exposing the underlying AlZnAg alloy to further electrochemical degradation. As expected, alloys with chemical composition of 3.5 and 4.5 % Ag had the highest  $\text{AgZn}_3$  phase precipitate, as can be seen in table 3, which reported the highest corrosion rates. This means that the electrochemical degradation is influenced by chemical composition, and silver alloying element. Furthermore, an additional consideration should be pointed for the alloy with 4.5 wt. % Ag, which exhibited an unexpected electrochemical degradation rate. In agreement to the trend shown in Figure 2, the highest silver content in the AlZnAg alloy should have showed, both the highest weight loss and the highest corrosion rate; however, results along the test did not display this performance; in contrast, the AlZnAg alloy with 4.5 wt. % Ag enhanced its corrosion resistance compared to the alloy with 3.5 wt.% Ag. This behavior is probably associated to the fact that 4.5 wt. % Ag decreased the solubility of Zn within the Al matrix. Based on this statement, we considered that the solute-depleted zone is susceptible to sustained attack, and that an increment in size of  $\text{AgZn}_3$  particles

that reduces the amount of  $AgZn_3$  precipitates. This interpretation makes consistency with Saad et al., who reported an improvement of the oxidation resistance when Ag is added to the Zn-Sn eutectic alloy [21]. It was observed, that the addition of silver microconstituent in the AlZn alloy, influences with an increment of the Zn solubility in the solid solution of Al matrix, and decreases the Zn-rich phase.

**Table 3.** Relationship between silver composition and  $AgZn_3$  phase content on AlZnAg alloys

Alloy type	$AgZn_3$ phase content (%)
<b>Ag1</b>	0.00
<b>Ag2</b>	0.58
<b>Ag3</b>	1.93
<b>Ag4</b>	1.21

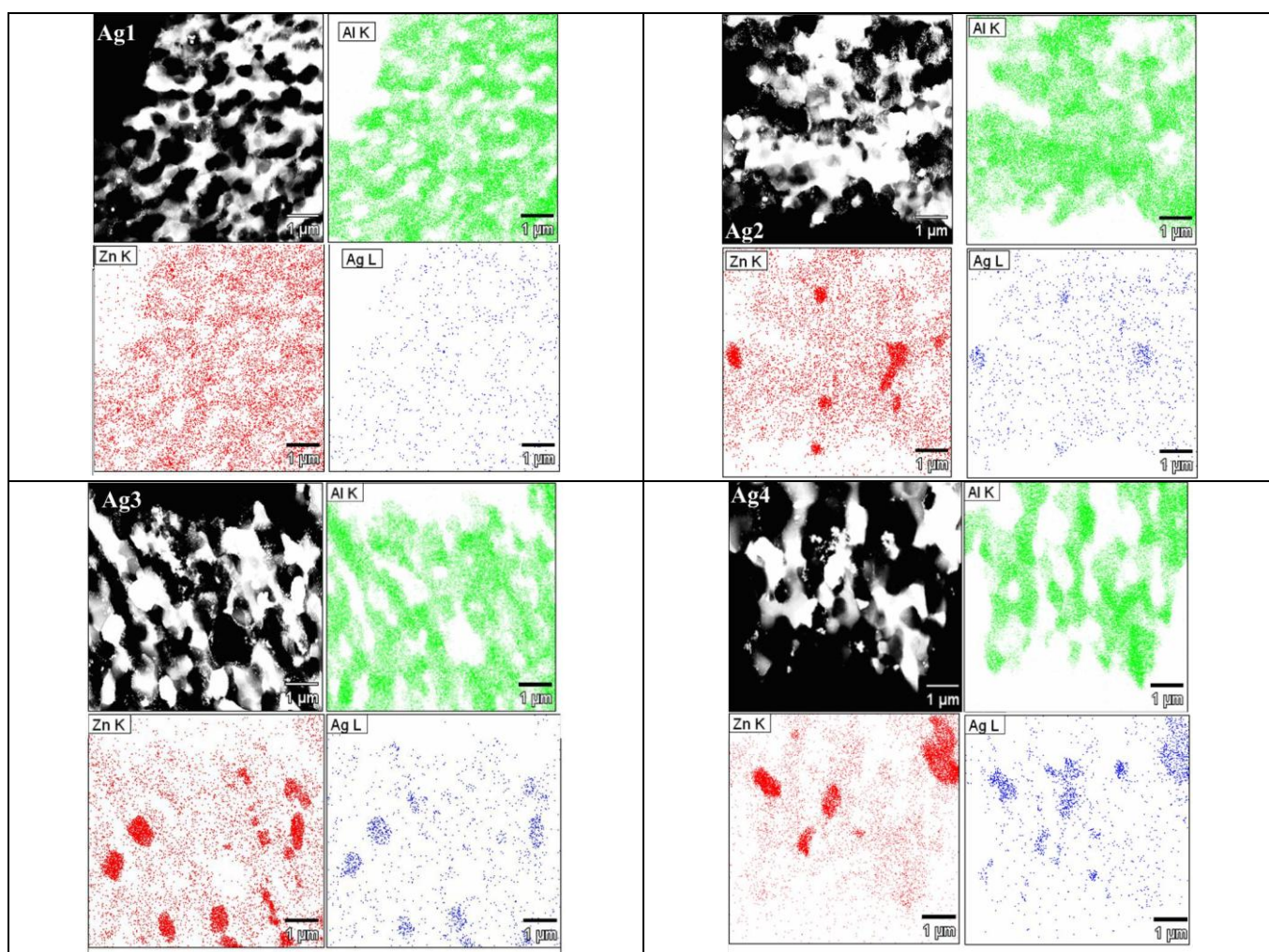


**Figure 3.** Elemental mapping distribution in AlZnAg alloys.

It is well suited dictate that microstructure is more meaningful for electrochemical degradation because microstructure involves both atom nature and, chemical composition. When the solidification

of AlZnAg alloy has been completed the final microstructure can be extremely complex. More than one phase can be responsible for the selective dissolution during the electrochemical reactions. For this reason, the Figure 3 shows the electron probe microanalysis of element distribution in AlZnAg alloys. The atom nature distribution was obtained by TEM with energy dispersive X-ray Spectrometer. As we know, the primary microstructure, second phases and precipitates can be anodic or cathodic as a result of selective dissolution. Precipitates identified by EDS which was built in the transmission electron microscope, has been identified as  $\text{AgZn}_3$ . As result, in the figure 3 with Ag2, Ag3 and Ag4 could be observed that the  $\text{AgZn}_3$  precipitation occurs when the silver composition was  $>2.5$  wt.%. Here when the Ag content is less than 2.5 wt.%, the silver atoms are dissolved into the solid solution phase Zn-rich (Figure 3-Ag1 ). Work on to emphasize the silver influence onto microstructure, the Figure 3-Ag3 shows the precipitates  $\text{AgZn}_3$  for 3.5wt.% Ag addition. Which is associated with three times more precipitates than the 2.5 and 4.5 wt.% Ag. It can be seen that the content of silver as solute microconstituent is high, and its distribution is chemically homogeneous for the figure 3 (Ag1, Ag2, Ag3 and Ag4) alloys. Is well known that the alloying elements distribution, either in solid solution or as second-phase particles, intermetallic compounds or inclusions, depend on the casting conditions used.

In the case of silver as microconstituent alloying, the electrochemical properties and metallurgical microstructure are also related with silver chemical concentration. In the figure 3(Ag1, Ag2, Ag3 and Ag4) it can be observed that the silver element as solute is less distributed with the  $\text{AgZn}_3$  phase increases. In addition, we can observe enrichment zones, which correspond to the  $\text{AgZn}_3$  precipitates. With the increase in Ag content, the amounts, and size of  $\text{AgZn}_3$  also increase.

#### 4. CONCLUSION

- The silver addition improves the formation of a passive region. The positive effect is more evident at 3.5 wt% Ag contents.
- The  $\text{AgZn}_3$  precipitate activates the electrochemical degradation process of the AlZnAg. The amount of precipitate is influenced by the Ag chemical concentration.
- The silver addition up to 3.5 wt. % clearly increased the degradation rate but it induced a passive region.

#### ACKNOWLEDGEMENTS

The present project is supported by DGAPA-UNAM program Award No. PAPIIT-IN105708, and by CONACyT program Award No. 167583.

#### References

1. D. V. Alexandro, A. P. Malygin. *Inter. J. Heat Mass Transfer*. 55 (2012) 3755.
2. Hiroshi Kato, Yukihiko Ando. *Mater. Trans*. 52 (2011) 179.
3. V. A. Hosseini, S. G. Shabestari, R. Gholizadeh. *Mater. Design*. 50 (2013) 7.

4. Jin-long Wang, Fu-ming Wang, Yan-yu Zhao, Jion-ming Zhang, Wei Ren. *Inter. J. Minerals, Metall. Mater.* 16 (2009) 640.
5. M. Asta, C. Beckermann, A. Karma, W. Kurz, R. Napolitano, M. Plapp, G. Purdy, M. Rappaz, R. Trivedi. *Acta Mater.* 57 (2009) 941.
6. Tao Zhou, Hua Xia, Mingbo Yang, Zhiming Zhou, Kang Chen, Jianjun Hu, Zhenhua Chen. *J. Alloys Comps.* 509 (2011) L145.
7. Temel Savaskan, Ali Pasa Hekimoglu, Gencaga Purcek. *Tribol. Inter.* 37 (2004) 45.
8. Bondan T. Sofyan, K. Raviprasad, Simon P. Ringer. *Micron* 32 (2000) 851.
9. D. Bakavos, P. B. Prangnell, B. Bes, E. Eberl. *Mater. Sci. Eng.* A491 (2008) 214.
10. Ying Deng, Zhimin Yin, Kai Zhao, Jiaqi Duan, Jian Hu, Zhenbo He. *Corr. Sci.* 65 (2012) 288.
11. Chaitanya Sharma, Dheerendra Kumar Dwivedi, Pradeep Kumar. *Mater. Desig.* 43 (2013) 134.
12. American Society for Testing and Materials, ASTM G31-72: Standard Practice for Lab immersion Corrosion Testing of Metals, 1999.
13. Standard Specification for Substitute Ocean Water, ASTM D1141-75.
14. Metehan C. Turhan, Qianqian Li, H. Jha, Robert F. Singer, Sannakaisa Virtanen. *Electrochim. Acta* 56 (2011) 7141.
15. X. L. Zhang, Zh. H. Jiang, Zh. P. Yao, Y. Song, ZhD. Wu. *Corr. Sci.* 51 (2009) 581.
16. K.H.Lo, C.H.Shek, J.K.L.Lai. *Mater. Sci. Eng.* R65 (2009) 39.
17. Jiuba Wen, Junguang He, Xianwen Lu. *Corr. Sci.* 53 (2011) 3861.
18. Wislei R. Osório, Pedro R. Goulart, Amauri Garcia. *Mat. Lett.* 62 (2008) 365.
19. A.A. El-Meligi. *Inter. J. Hydr. Ener.* 36 (2011) 10600.
20. Xianghoung Li, Shuduan Deng, Hui Fu, *Mater. Chem. Phys.* 115 (2009) 815.
21. G. Saad, A. Fawzy, E.J. Shawky, *Alloys Comps.* 479 (2009) 844.